Interpreting Artificial Neural Network Output for the Microwave Detection of Breast Cancer

Douglas A. Woten [1], Magda El-Shenawee[1], and John Lusth [2]

[1] Department of Electrical Engineering
University of Arkansas, Fayetteville, AR 72701, USA
dwoten@uark.edu , magda@uark.edu

[2] Department of Computer Science and Computer Engineering
University of Arkansas, Fayetteville, AR 72701, USA
lusth@uark.edu

Abstract: The applicability of Artificial Neural Networks to breast cancer detection is explored in this work. A simplified model of the breast containing a tumor is used and the scattered electromagnetic waves are used to train and test a series of networks with noise introduced to into the input signal. Two methods of interpreting the output signal of the network are explored and the results presented.

Keywords: Breast Cancer Detection, Artificial Neural Networks, Wave Scattering

1. Introduction

Breast cancer, according the American Cancer Society, will be responsible for over 40,000 deaths in 2006 alone. For women between under the age of 54 it is the leading cause of cancer related deaths, and is second only to lung related cancer deaths for women over 54. Additionally, more than 1.7 million women diagnosed with breast cancer are alive in the United States today [1]. The survival rate of a patient diagnosed with breast cancer is inversely related to the time taken before diagnosis, as treatment is most effective in the early stages. X-ray mammography is the current standard for breast cancer screening. Mammography, however, suffers from false negative rates as high as 34% [2], and relies on the ability of the doctor to physically observe abnormalities. In response to these limitations, microwave imaging has emerged as a possible solution, allowing a safe and effective diagnosis.

The potential of microwave imaging is due to the significant contrast in electrical properties between the tumor and healthy breast tissue at microwave frequencies. This contrast has been shown to be on the order of 10-1 [3]. This large contrast allows for the detection of smaller tumors than traditional methods with a high accuracy [4,5]. An additional benefit of this method is that the patient is not exposed to ionizing radiation. Microwave systems are typical designed for detection or imaging, each having their own requirements. Detection seeks to determine whether an abnormality is present in the breast, while imaging requires a high degree of spatial resolution to determine the exact location and shape of an abnormality [6,7].

Imaging algorithms rely on an iterative process that seeks to refine the shape and location of an object over many passes. This process is time intensive and requires a great deal of computational resources. This paper shows the feasibility of using an Artificial Neural Network (ANN) as a rapid breast cancer detection method.

The network can then be used as a preprocessor to the time intensive imaging algorithms. The goal is to reduce the number of cases unnecessarily passed to the imaging algorithm.

2. Methodology

For this work the breast is modeled as a homogeneous region containing a tumor. An incident plane wave with vertical polarization is used as seen in Figure 1. In this study the skin layer is ignored. Studies have been conducted on the effect of ignoring the skin layer from various transmitting and receiving locations [8]. For backscatter this error is approximately 3%. The dielectric properties for healthy breast tissue and breast tumor were randomly chosen from the ranges reported in the literature [3]. Perfect matching between the medium outside the breast and the breast tissue is assumed.

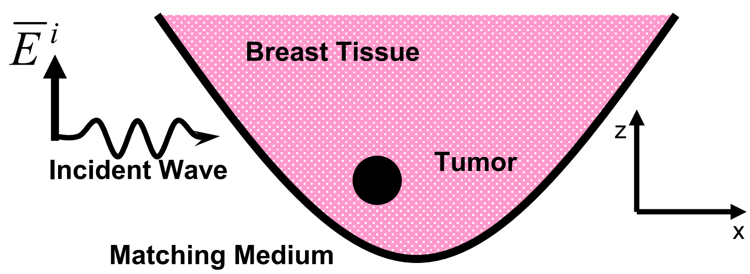

Figure 2: Model of the breast and incident plane wave at 6GHz with tumor of radius 5mm.

The scattered electromagnetic fields (E_x, E_y, and E_z) from a tumor of radius 5mm is calculated using code based on the Method of Moments (MoM) [6]. This is repeated 100 times for different dielectric values for cases with a tumor, and again for cases without a tumor (total of 200 cases). The data is then divided into a training set and a testing set, each comprising 50 cases with a tumor and 50 cases without a tumor. Synthetic variations (noise) is added to each set based on a Gaussian distribution with mean of zero and varying standard deviations, σ_n (σ_n = 0.001, 0.01, 0.1, 0.2, and 0.3) The effect on the real component of E_x by the introduction of noise can be seen for two cases in Figure 2.

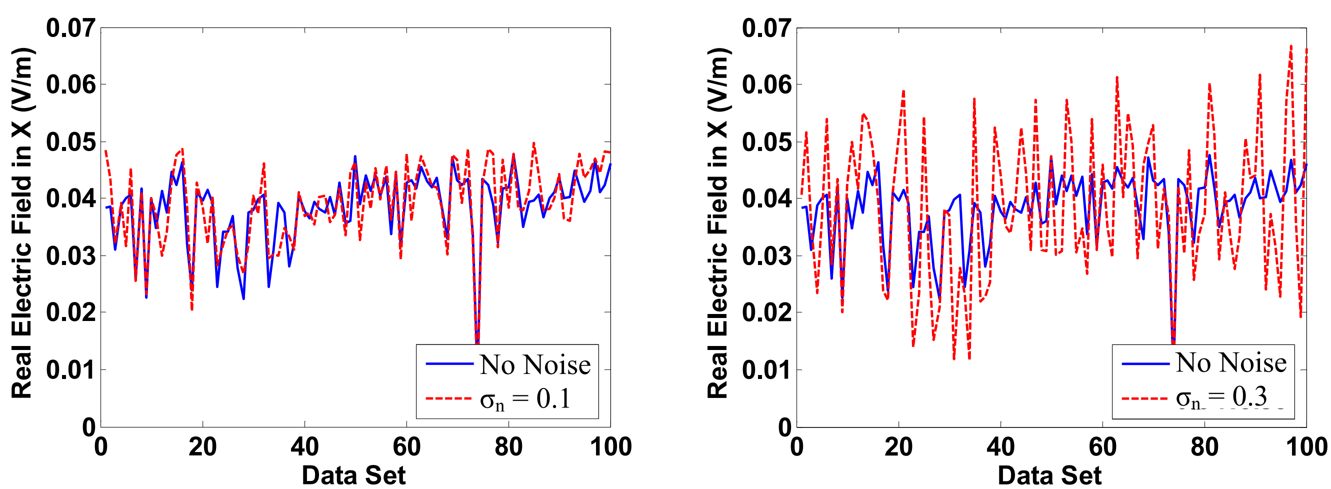

Figure 2: Demonstration of noise on Re(E_x) and Im(E_x) plotted vs. data sets.

An ANN is a processing technique loosely based on the human brain in which interconnected layers processing information simultaneously and adapt over the course of multiple runs [9]. Typical ANNs consist of an input layer, a hidden layer, and an output layer. Each layer is composed of any number of nodes which are connected to nodes in the other layers. For this work the input layer consists of six nodes corresponding to the real and imaginary parts of E_x, E_y, and E_z. The hidden node contained two nodes to minimize the complexity of the network while still allowing acceptable accuracy. The output layer contained a single node. This network is fully interconnected.

At each node, an activation function is called to manipulate the inputs from previous nodes. Activation functions can take many forms dependent on the desired output, and this work used a saturation function to constrain the network output between 0 and 1. The function is given by:

$$f(x) = 1/\left(1 + e^{-\beta x}\right). \tag{1}$$

Where β is a constant determining the slope of the function and is determined during the iterative error minimization process by the ANN.

For this project the package NevProp 3 – Nevada backPropagation Version 3 is used (open source). A fully interconnected network with two nodes in the hidden layer is implemented using this package.

3. Results

The ANN was training on the one hundred cases in the training set, and then tested against the one hundred cases in the testing set. This produced one hundred values between 0 and 1, corresponding to the network's determination of whether a tumor existed or not. At this stage a cutoff value must be selected which will determine what outcomes constitute the presence or absence of a tumor. Two schemes were implemented and the results compared. The first method uses a single cutoff value which divides the data into two possible outcomes, 1) a tumor is present and 2) no tumor is present. The second scheme uses a double cutoff to divide the output data into three categories, 1) a tumor is present 2) undecided and 3) no tumor is present. By comparing the predictions of the ANN against the known presence/absence of a tumor the networks accuracy can be determined.

To determine the optimum cutoff(s), Receiver Operating Characteristic (ROC) curves are implemented. A ROC curve is a graphical representation of the trade off in the false negative and false positive rates for every cutoff. By varying the cutoff value for each test and calculating the number of false positives and false negatives, ROC curves are created (Figure 3). The probability of detection is defined as ($1 - FalseNegativeRate$).

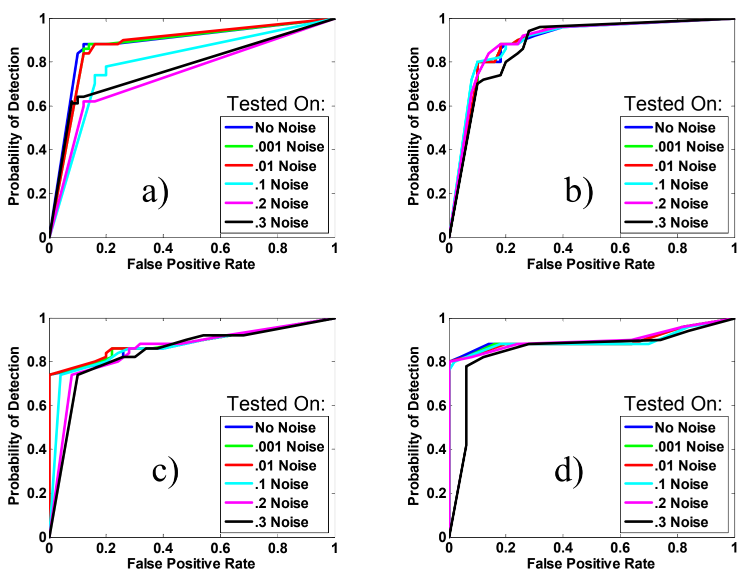

Figure 3: The probability of detection vs. the false positive rates for training on a) No Noise, b) $\sigma_n = 0.1$, c) $\sigma_n = 0.2$, and d) $\sigma_n = 0.3$.

The accuracy of the test is measured as the area under the ROC curve. An ideal diagnostic test would climb straight to 1 on the y-axis and the area under the curve would be 1. Figure 3 shows that as the amount of noise in the testing set is increases, the ANN becomes less accurate. As the level of noise increases in the training set, however, the ANN performs progressively better and more consistently. Figure 3 d) shows the best performance of the network. This is in agreement with the findings of Wang *et al* who showed that introducing additive noise into the input signal increased the robustness of an ANN [10]. The ideal cutoff would correspond to the cusp of the ROC curve in which the tradeoff between accuracy and false positives is low.

To determine this optimal cutoff Youden's Index, a method to minimize false positives and false negatives, is used [11]. The standard form of Youden's Index, Y, is given by:

$$Y = 1 - \left[(FNR) + (FPR)\right]. \tag{2}$$

Where FNR represents the false negative rate and FPR represents the false positive rate.

Youden's index is found for the cutoffs corresponding to multiples of 0.1 (i.e. 0, 0.1, 0.2, 0.3, etc…) and the cutoff corresponding to the highest index is recorded for each case. The optimum cutoff was chosen to be the average of the individual cutoff values with the highest index, Y. This optimum cutoff was found to be 0.6. Using this optimum cutoff the number of false positives, false negatives, and correctly identified results are tabulated and plotted. Figure 4 depicts the results obtained for varying training sets when tested against a data set with $\sigma_n = 0.1$.

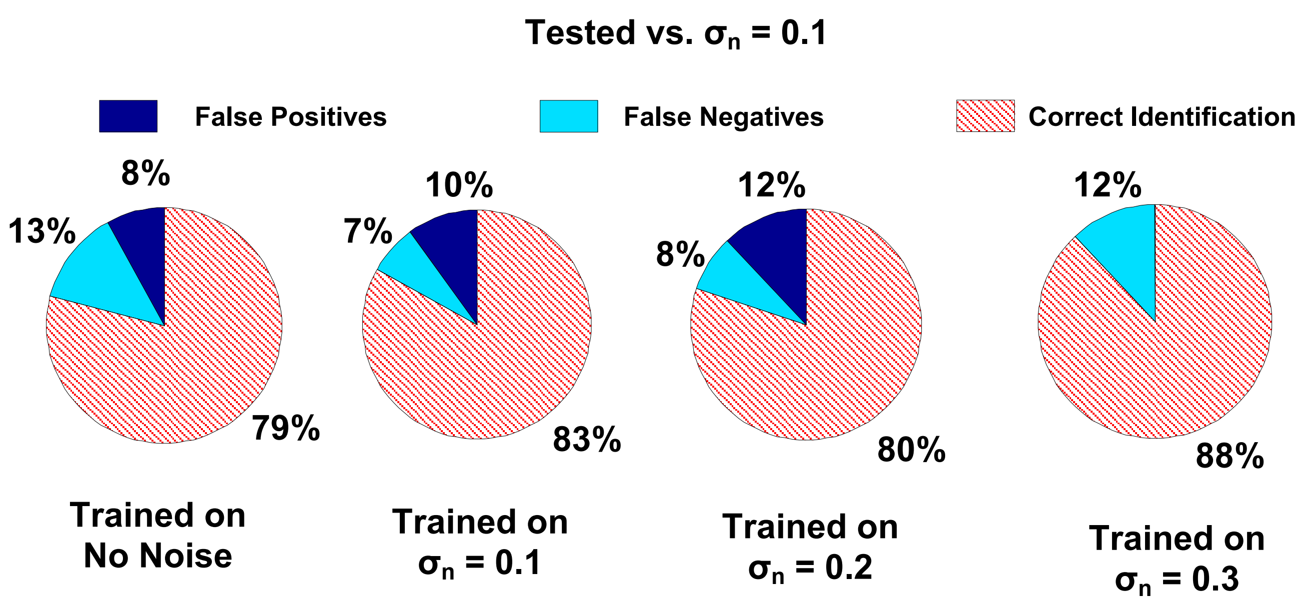

Figure 4: Pie charts for varying training sets when tested against the testing set with $\sigma_n = 0.1$ using a single cutoff.

It is clear from Figure 4 that the introduction of noise into the input signal of the ANN did improve on the overall accuracy of the network as mentioned previously. The trend implies that as the noise is increased the network performance increases simultaneously. There is, of course, a point at which this trend reverses and the introduction of more noise is detrimental to the network's performance. For noises around 0.5 and above the network does not perform well.

Youden's Index is unbiased towards the FNR and the FPR by formulation, since both are weighted with a value of 1. Although the ultimate goal for breast cancer detection is a method that eliminates both false positives and false negatives, one could argue that false negatives are far worse than false positives. A false positive will potentially subject a patient to a great deal of stress, a false negative can mean that a tumor goes untreated and is a threat to a patient's health. Additionally, it is arguable that an inconclusive result is better than an incorrect result. For these reasons it is beneficial to use a modified version of Youden's Index that utilizes a weight scheme to manipulate the optimal cutoff value, and to determine two distinct cutoff values. The output that falls between these two cutoff values corresponds to an undecided result. It has been shown that weights can be added to Youden's Index corresponding to the severity of the FNR and FPR. The modified version of Youden's Index is given by [11]:

$$Y = 1 - \left(w_{sens} FNR + w_{spec} FPR \right). \tag{3}$$

Where w_{sens} is the weight associated with the sensitivity and w_{spec} is the weight corresponding to the specificity.

For this work the weights were chosen somewhat arbitrarily as there is no quantitative measure of how much worse a false negative is than a false positive. To minimize the number of both the false positives and false negatives the weights are chosen to be 1 and 2 and the optimal cutoff is found as before. The weights are then changed to 2 and 1 and the resulting optimal cutoff is found. These two cutoffs are used for the double cutoff scheme. They were found to be 0.5 and 0.9. Using these cutoffs the number of false positives, false negatives, undecided, and correctly identified results were tabulated. Figure 5 depicts the results for the same cases as Figure 4 with the number of undecided results included.

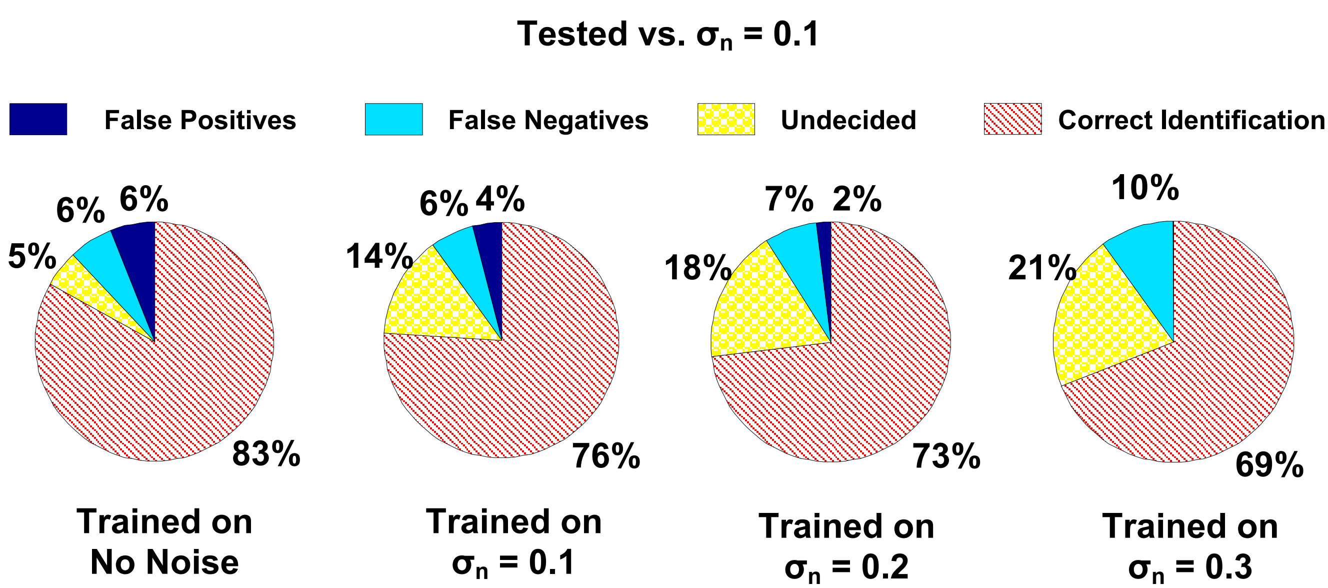

Figure 5: Pie charts for varying training sets when tested against the testing set with $\sigma_n = 0.1$ using a double cutoff.

Comparing figures 4 and 5 it appears that the introduction of undecided results decreases the accuracy of the network. This decrease in accuracy, however, accompanies a decrease in the number of false positive and false negative results. Additionally, the level of noise in the training set seems to directly correlate to the number of undecided results present. This would imply that as the level of noise in the training set increases, the ability for the network to provide output at the extremes decreases and the number of outputs nearer the center of the distribution increases.

Work is in progress to develop a realistic model of the breast containing a skin layer and an inhomogeneous medium. The transmitting and receiving elements are based on real antennas and the results will be presented.

4. Conclusions

Two methods for interpreting ANN output have been presented in the context of breast cancer detection and the advantages and disadvantages of each have been discussed. In the worst case results (highest level of noise in the training and testing set using a double cutoff) the accuracy of the network was 68%, corresponding to an inaccurate diagnosis rate of 32% on the simplified model. This is comparable to the worst case results reported in the literature for mammography, of 34%.

The inherent adaptability of ANNs allow for a great degree of flexibility in their configuration while still providing results in a mere milliseconds. Additionally, by manipulating the cutoffs according to what the situation dictates ANNs are a potential candidate as a preprocessor to imaging algorithms. By setting the cutoffs arbitrarily low, the number of false negatives can be reduced to zero while increasing the number of false positive and undecided results. Since the false positives and undecided results would be passed to the imaging algorithm regardless, there is no penalty for such a system.

When this system was implemented with the highest noise in the training and testing sets ($\sigma_n = 0.3$) and the cutoff set to 0.1, the network was able to correctly diagnose 20% of the cases with no tumor present. This means that if implemented this system would have saved 10% of the total cases from being passed to the imaging system unnecessarily. Due to the real time results of the network there is no significant cost or penalty for implementing such a system.

5. Acknowledgements

This work funded in part by the National Science Foundation GK-12 Program, National Science Foundation Award Number ECS – 0524042, the Arkansas Biosciences Institute, and the Women's Giving Circle at the University of Arkansas.

References

[1] American Cancer Society. Cancer facts and figures 2006. Atlanta: American Cancer Society; 2006.

[2] P. T. Hunynh, A. M. Jarolimek, and S. Daye, "The false-negative mammogram," *Radiograph*., vol. 18, no. 5, pp. 1137-1154, 1998.

[3] S. Gabriel, R. W. Lau, and C. Gabriel,"The dielectric properties of biological Tissues-II: Measurements on Frequency range 10 Hz to 20 GHz," *Phys.Med.Bio,* vol 41, no. 11, pp. 2251-2269, Nov. 1996.

[4] P. M. Meaney, M. W. Fanning, Dun Li, S.P. Poplack and K.D. Paulsen, "A clinical prototype for active microwave imaging of the breast," *IEEE Trans.Microwave Theory Tech.*, vol. 48, pp. 1841-1853, 11/.2000.

[5] E.J. Bond, Xu Li, S.C. Hagness and B.D. Van Veen, "Microwave imaging via space-time beamforming for early detection of breast cancer," *IEEE Transaction on Antennas and Propagation*, vol. 51, pp. 1690-705, 08/.2003.

[6] M. El-Shenawee and E. Miller, "Spherical Harmonics Microwave Algorithm for Shape and Location Reconstruction of Breast Cancer Tumor," *IEEE Transaction on Medical Imaging*, vol 25, pp 1258-1271, 10/.2006.

[7] P. Rashidi, "Microwave Imaging for Breast Cancer Based on Evolution Strategies," M.S. thesis, University of Arkansas, Fayetteville, AR, USA, 2006.

[8] S. Pandalraju, "A Hybrid Algorithm Based on Mie Theory and Evolution Strategy for Breast Cancer Imaging," M.S. thesis, University of Arkansas, Fayetteville, AR, USA, 2006.

[9] D.E. Rumelhart, G.E. Hinton, and R.J. Williams, "Learning Internal Representations by Error Propagation," *Parallel distributed processing: Explorations in the microstructure of congnition*. vol. 1 1986.

[10] C. Wang and J. Principe, "Training Neural Networks with Additive Noise in the Desired Signal," *IEEE International Conference on Neural Networks*, Anchorage, AK, 7/.1998.

[11] A. Kristopher L., Pretty, Ian A, Results of the 4th ABFO Bitemark Workshop – 1999, *Forensice Science International*, vol. 124, pp. 104-11.